EXPERIMENTAL AND NUMERICAL INVESTIGATION OF A PILOT STEEL LADLE

Pratik N. Gajjar, João M. Pereira, Paulo B. Lourenço
University of Minho, ISISE, ARISE, Department of Civil Engineering, Guimarães, Portugal

Pieter Put, Bruno Luchini, Sido Sinnema
Ceramics Research Centre, Tata Steel, 1951MD Velsen Noord, The Netherlands

ABSTRACT

Masonry refractory linings are commonly employed in industrial vessels to protect against extreme working environments. Mortarless refractory masonry is frequently used in the working lining of steel ladles to contain the molten steel and limit heat losses. During operation, such masonry lining undergoes high thermo-mechanical loads, primarily due to the complex thermal and mechanical boundary conditions. Therefore, large-scale experiments are required to characterise the behaviour of such structures, leading up to their optimisation. This work presents a novel approach for the experimental characterisation of refractory linings using a laboratory-scaled pilot steel ladle. This 3D pilot model is a scaled representation of a ladle that includes all the linings as an industrial ladle. The pilot ladle was tested under transient thermal loads, and its behaviour was assessed through thermocouples, strain gauges and DIC (digital image correlation). The experimental observations describe a complex and nonlinear global behaviour of the pilot ladle due to thermal gradient, creep of the refractories and damage. Finally, the results obtained from these experiments were used to validate numerical models using a 3D meso-modelling approach. The numerical simulations revealed a good agreement with the experimental outcome that can further be employed to investigate and design an industrial steel ladle.

1. INTRODUCTION

Steel ladles play a crucial role in the steelmaking industry. They are employed as industrial vessels to transport and refine molten steel and are exposed to a harsh operating environment. Normal operating conditions of these vessels include high temperatures, high thermal stresses, slag attack, and degradation of layers in contact with molten steel [1]. Steel ladles are often built with multiple layers of refractory masonry linings enclosed within a thick steel shell to withstand extreme operating conditions. Each layer comprises refractory materials with different thermal, mechanical, and chemical properties. The selection of refractory materials for these layers depends on their designed purpose, such as thermomechanical behaviour, thermal insulation, and chemical stability. Therefore, knowledge of the thermal, mechanical, and chemical behaviour of the refractories becomes essential to optimise their consumption in extreme working environments.

The working lining of a steel ladle is usually constructed with mortarless masonry. The joints of such masonry provide a physical break in continuous media, which can reduce the stress build-up. These dry joints show a high nonlinear behaviour affected by material type, contact area distribution, and the spatial and size distributions of the asperities on the surfaces [2]. Therefore, large-scale experimental campaigns are required to evaluate the global behaviour of refractory masonry under varying thermal and mechanical boundary conditions. These campaigns also validate the material properties derived from experiments at material levels, noting that limited work is available in the literature regarding the large-scale experimental evaluation of such masonry.

Oliveira et al. [3] experimentally investigated the mechanical behaviour of mortarless refractory masonry under uniaxial compression with various loading conditions at ambient and high temperatures (900°C). Their work highlights the heterogeneity in mortarless refractory due to dry joints and its influence on thermomechanical behaviour, which is widely used in steel ladles. Further, Ali et al. [4] evaluated the mechanical behaviour of the mortarless refractory masonry in a biaxial press under various loading and boundary conditions at ambient and high temperatures (1500°C). They observed permanent deformation of bricks due to viscoplastic behaviour. This experimental campaign shows the presence of viscoplasticity in alumina spinel bricks at high temperatures and its impact on refractory masonry under different loading conditions. Gasser and Poirier [5] investigated the thermomechanical behaviour of mortarless refractory masonry in a laboratory pilot that resembles a steel ladle. The test was conducted with only one layer of refractory lining and was performed under transient thermal loading with a maximum temperature of 1000°C. They observed that the elastic strains observed from the steel shell reveal the thermomechanical behaviour of the refractory lining. The behaviour of the lining was influenced by the dry joints present and the contact between the bricks and steel shell.

Finite element models are often used to investigate or design industrial installations such as steel ladles with different linings of refractory masonry. The data obtained through experimental campaigns are used to calibrate models with varying degrees of complexity from linear thermo-elastic to more complex models, including viscoplasticity and damage [1,6,7]. However, the behaviour obtained through such models for a steel ladle is not validated due to a lack of experimental investigations. Therefore, experimental work must be carried out to validate numerical models on an assembly representing an industrial ladle subjected to a thermal loading similar to normal operating conditions (around 1500°C).

This work presents a novel experimental setup for large-scale refractory masonry to characterise a pilot steel ladle that undergoes similar thermomechanical loadings as an industrial ladle to gather data to validate numerical models.

2. DEVELOPMENT OF THE PILOT LADLE

The scale of the pilot ladle should be such that it is small enough to be handled at the laboratory level and big enough to represent the global behaviour of an industrial ladle. The other difficulties involved with the scale are the thickness of the steel shell and the size and shape of the refractory bricks. To tackle these challenges, preliminary numerical investigations were developed, assisting with the design and, ultimately, contributing to the choices made regarding the installation itself. From the design optimisation process, only the barrel part of the ladle with 1500 mm diameter and 500 mm in height was made, as shown in Fig. 1. This configuration contains all refractory linings with identical lining thickness as in industrial ladle enclosed within a 6 mm thick steel shell.

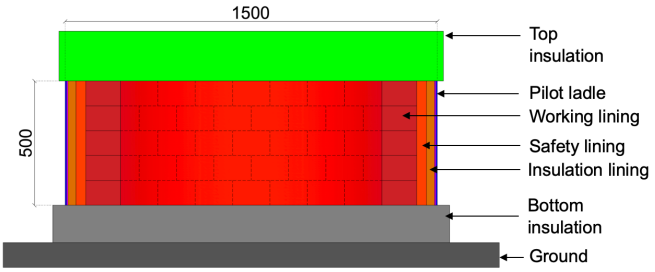

Fig. 1: Graphical illustration of the pilot steel ladle showing pilot ladle, refractory linings, and top and bottom insulation.

The working lining is made of mortarless masonry with alumina spinel bricks, providing good thermal, chemical and mechanical stability at high temperatures. The safety lining is constructed with bauxite brick, offering better thermal insulation than working linings with good mechanical behaviour. Insulation lining is used to reduce the heat losses in the ladle. The material used in this lining is aluminium silicate which has low thermal conductivity. The insulation board is an additional lining component to further reduce

heat losses. This microporous material offers excellent thermal properties while it is highly compressible.

For the measurement of thermal fields, thermocouples were used. An assembly of thermocouple placement was installed at three different locations and layers of the pilot ladle (spaced at about 120º in the plan view), as shown in Fig. 2 (total of 18 thermocouples). Six type K thermocouples were installed in different refractory linings at one location. One type S thermocouple was placed near the innermost part of the working lining. Additional thermocouples were placed inside the bottom insulation layers to monitor the heat losses.

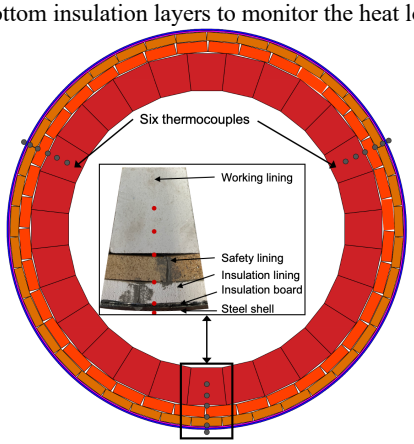

Fig. 2: Placement of thermocouples to measure thermal fields.

DIC was employed to monitor displacement and strains in the working lining through a cut window in the top lid and on the exterior section of a steel shell. Additionally, three high-temperature spot welding foil strain gauges from Kyowa (self-temperature compensating) were placed on the structure's cold face, close to the thermocouples shown in Fig. 2.

3. EXPERIMENTAL RESULTS

Fig. 3 shows the final experimental setup of the pilot steel ladle with all components and measurement devices. Two tests were performed on a pilot with new working linings (NWL) by applying thermal load through 18 heating elements. Once the target temperature was achieved, an eight-hour dwell time was used for all the tests. The test specimen NWL-01 was tested till 1250°C to check the structural safety of the pilot ladle, while the other test reached 1400ºC. This experimental device was constructed and tested at the Ceramics Research Centre (CRC) of Tata Steel in Ijmuiden, Netherlands.

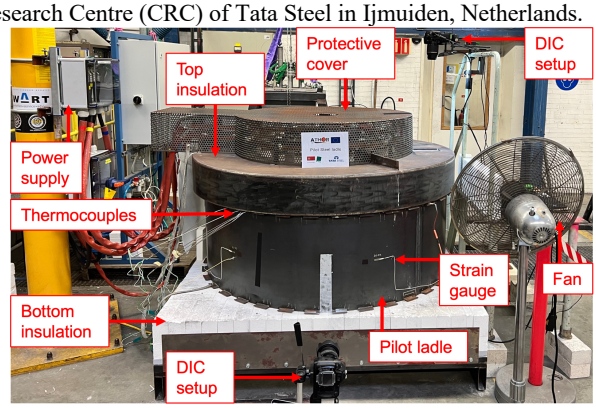

Fig. 3: Experimental setup of the pilot ladle.

Fig. 4 shows the average temperature evolution observed in the installed thermocouples at various heights. At the beginning of the thermal loading through heating elements, the whole assembly of the pilot ladle was at room temperature of around 16°C. The thermal loading was applied at a rate of 4°C/minute. It is possible to notice that the applied rate of thermal loading was sustained till 500°C of the furnace temperature. Afterwards, the rate of loading decreased due to increased power requirement. However, at the 20th hour, the furnace temperature reached 1250°C for both tests. For the test specimen NWL-01, the applied temperature was kept constant for the next eight hours, and for the other test specimen, the applied temperature was increased to 1400°C. Once the 1400°C desired temperature was achieved at the 36th hour, the same was kept constant for the next eight hours.

For both specimens, temperature evolution observed in the linings is very similar. Moreover, irregular temperature evolution can be observed at the different linings at 100°C, which can be attributed to the evaporation of free water. The temperature evolution and distribution in the ladle linings exhibit the expected thermal behaviour of a steel ladle. Temperature measurement data provides insight into the behaviour of different layers in the lining when applying thermal loads. Considering the selection of materials used in the linings and their different thermal properties, a complex temperature distribution from the hot face to the exterior of the steel shell can be observed.

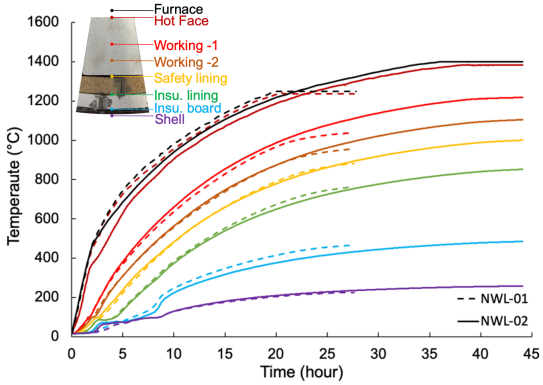

Fig. 4: Average temperature evolution observed during experiments.

As mentioned, the working lining is built with dry joints. Therefore, measurements were taken before and after the experiments on both specimens to observe the change in the joint thickness. Tab. 1 presents the measurements taken for the head joint at the hot face. The influence of the dry joint on the global behaviour can be observed through the strain gauges installed on the outer steel shell.

Tab. 1:Change in the thickness of head joints.

	NWL-01		NWL-02	
	Before	After	Before	After
Mean joint thickness (mm)	0.32	0.40	0.23	0.47
Standard deviation (mm)	0.30	0.26	0.27	0.31
Largest joint (mm)	1.68	1.46	1.77	1.25

The performance of the steel shell is a critical issue in the behaviour of the refractory linings subjected to thermal loads. Fig. 5 shows the average mechanical strain observed in the circumferential direction through strain gauges on the exterior surface of the steel shell. The strain evolution confirms a highly nonlinear behaviour during thermal loading. During the early stage of the test, a slight increase in the strain can be observed. This increase can be attributed to the closing of the head joints in the working lining as well as the closing of the gap between the linings. Once these joints are closed, a steady growth in the strain can be observed till about the 20th hour. The effect of the joint thickness can also be noticed from the maximum strain observed. NWL-02 exhibits stiffer behaviour compared to NWL-01. This difference was expected as the average head joint thickness in the working lining is smaller for NWL-02 (0.23 mm) compared to NWL-01 (0.32 mm). After the 20th hour, strain reduction can be observed till the end of the test. In NWL-01, the maximum applied temperature was lower (1250°C) than NWL-02 (1400°C). Therefore, during the dwelling period for NWL-01, no significant drop in strain was observed. However, for NWL-02, despite a rise in applied temperature after the 20th hour (consequently an increase in thermal expansion), a gradual reduction in the strain was observed (from 0.57 to 0.48 mm/m). This reduction is due to the viscoplastic behaviour of the alumina spinel bricks in the working lining that becomes prominent after 1200°C.

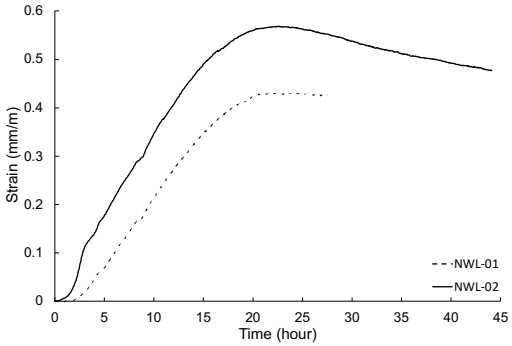

Fig. 5: Average circumferential strain evolution.

DIC analysis measures the total strain on an inspected surface. Under thermomechanical loading, the total strain comprises of elastic, thermal and inelastic strain. Fig. 6 shows the evolution of circumferential strain observed from DIC analysis on the steel shell. The figure also shows the expected thermal strain due to temperature rise in the steel shell and total strain (calculated thermal strain plus measured average strain from strain gauge). The total strain observed from the DIC shows similar behaviour as the calculated strain. The differences observed between the observed and calculated strain may be partly due to the hot air draft that affects the image captured by the camera, particularly when DIC values are lower.

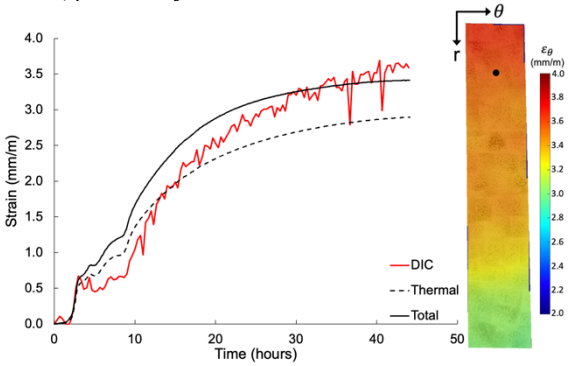

Fig. 6: Circumferential strain evaluation at 250mm height of the shell and strain distribution at the 44th hour.

Fig. 7 shows the evolution of the strains in the circumferential direction, measured at 25 mm and 130 mm from the hot face of the working lining brick. The values presented are the average strains observed from virtual extensometers at both bricks. The strain evolution shows an increase in strain at both locations as the temperature increases due to thermal expansion. The strain level observed at 25mm from HF is low compared to the expected 12 mm/m thermal strain. The difference is due to the combination of thermal expansion, onset of viscoplasticity and joint closing. However, the strain observed at 130 mm from HF is comparable with the thermal strain due to expansion at that location, 8.8 mm/m expected vs 7 mm/mm measured. This lower difference suggests less relevance of joint closing and no viscoplasticity at that location.

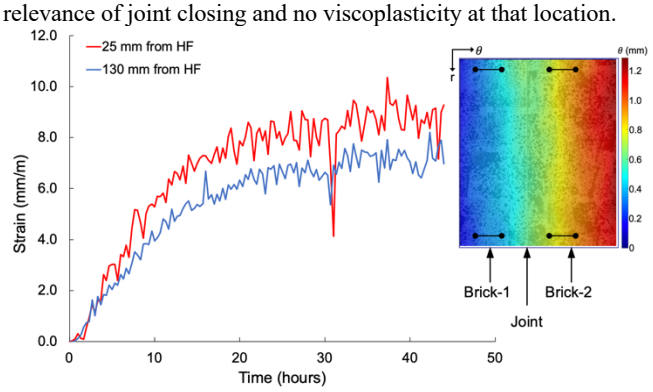

Fig. 7: Circumferential strain evaluation at 25mm and 130mm from the hot face and displacement distribution at the 44th hour.

4. VALIDATION OF NUMERICAL MODEL

Finite element models are often used to design or analyse steel ladles. Meso and macro modelling approaches are often used for this purpose. This work employed the meso modelling approach, where units (bricks) and joints are modelled separately. The model was made by taking advantage of the periodic geometry of the pilot ladle to reduce computational costs. Fig. 8 presents the 3D view of the meso model used and a plan view of the geometry showing the thicknesses of linings (mm).

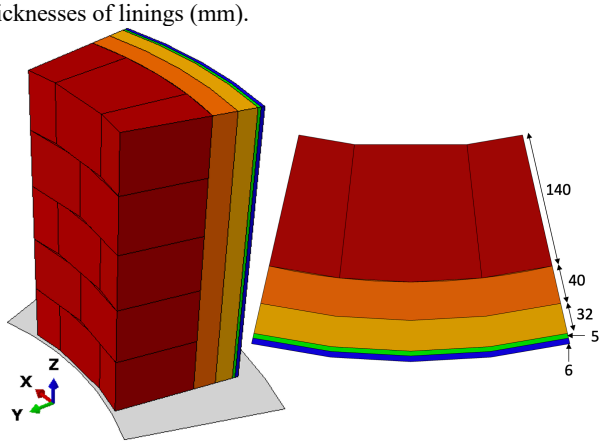

Fig. 8: FE meso model of pilot ladle showing the 3D and top view.

The analysis was performed using coupled thermal and mechanical analysis. The observed value of the furnace temperature was used as the thermal load at HF with a heat transfer coefficient of 600 W/m^{2}K. The exterior face of the steel shell was exposed to room temperature with a heat transfer coefficient of 50 W/m^{2}K. The thermal and mechanical properties of the materials were taken from [1,6]. For all the materials, temperature-dependent elasticity was used.

Additionally, the viscoplastic behaviour of the working lining was used. The measured value of head and bed joints from test NWL-02 was used in the model for the working lining masonry. These joints follow an exponential closure behaviour as described in [2]. The model was supported in gravity by a rigid plate (allowing separation in tension) and a friction coefficient of 0.7. The temperature distribution obtained with the numerical model shows good agreement with the experimental result, as shown in Fig. 9. The result validates the thermal properties of the materials used in the model.

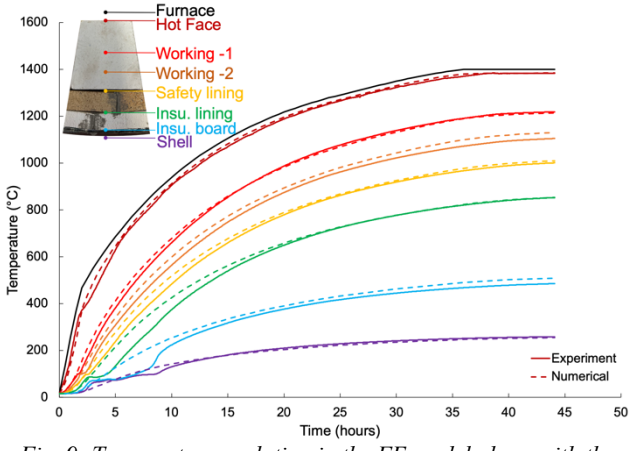

Fig. 9: Temperature evolution in the FE model along with the experimental result of NWL-02.

The evolution of circumferential strain in the steel shell of the FE model shows a good agreement with the experimental result, as shown in Fig. 10. The strain evolution can be expressed by the closing of the joints in working linings and gaps between the linings in the beginning. After joint closure, a steady rise in strain till the 20th hour, when the temperature at HF reaches 1200 °C. Afterwards, strain reduction can be observed. However, the drop in strain in the numerical model is not as prominent as in the experimental result.

This difference could be due to creep parameters used in the model, which requires further investigation.
Nevertheless, the obtained behaviour is well within the bounds of the experimental outcome. Fig. 10 presents the distribution of maximum principal creep strain in the working linings of the pilot. A strain concentration can be observed near the joints at HF, which is expected due to high-stress concentration. Higher creep strain can generally be noticed near the HF, and no creep at the CF of the working lining due to temperature distribution which influences the creep parameters.

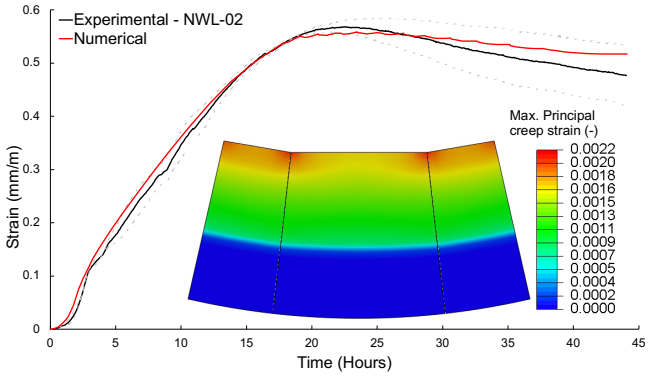

Fig. 10: Circumferential strain evolution in steel shell in FE model and experiment along with distribution of creep strain in working lining at the 44th hour.

Fig. 11 shows the evolution of total strain observed at the 25 mm from HF in working linings and the results obtained from the DIC analysis at that location. A good agreement between the results can be noticed. The figure also presents the total strain's thermal, elastic and creep strain components. As the applied temperature increases, a rise in thermal strain can be observed due to thermal expansion. After the joint closure, a build-up of elastic strain can be observed. An increase in the creep strain and, consequently, a reduction in the elastic strain can be observed once the temperature at that location reaches 1200 °C.

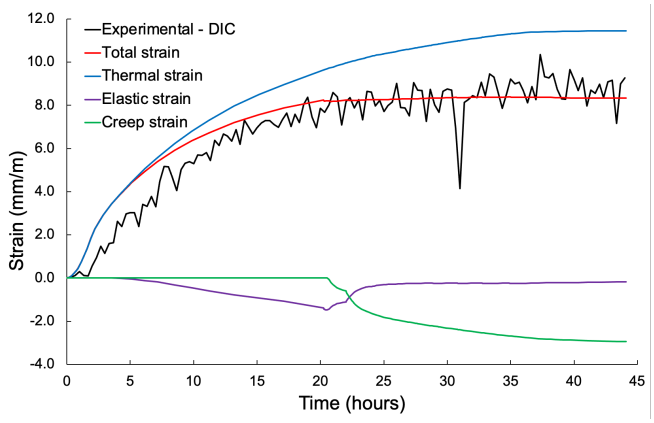

Fig. 11: Evolution of circumferential strain and DIC result.

5. CONCLUSION

Mortarless refractory masonry exhibits complex behaviour when subjected to high thermal loading, particularly with complex and multi-material industrial applications. Thus, characterising refractory masonry behaviour is essential for designing or investigating industrial vessels using it. Moreover, limited experimental works focusing on the thermomechanical characterisation of refractory masonry are available in the literature. This experimental campaign describes a novel simplified approach for the thermomechanical characterisation of a steel ladle's cylindrical shell without the constraints of ladle bottom and molten steel.
The thermal behaviour observed through various thermocouples presents a similar distribution of temperatures between the refractory linings for all tests. Tests performed on specimens with new working linings show the influence of evaporation of free water around 100 °C. The effect of the dry joint thickness can be observed by measuring mechanical strain in the circumferential direction on the exterior side of the steel shell. The working lining with a larger mean thickness of joints demonstrates lower strain on the steel shell than the lining with a small joint thickness. The effect of viscoplasticity that becomes prominent around 1200°C in working lining bricks was also observed through strain gauges on the steel shell.
The result presented here shows that the meso modelling approach provides a reliable response of the structure. This result also validates the various thermal and mechanical properties of the materials found in the literature. Moreover, this approach can be used to perform parametric analysis to identify critical material and geometric properties. Furthermore, the experimental and numerical outcome of this work can be used to validate other modelling approaches, such as homogenised macro models.

ACKNOWLEDGEMENT

This work was supported by the funding scheme of the European Commission, Marie Skłodowska-Curie Actions Innovative Training Networks in the frame of the project ATHOR - Advanced THermomechanical multiscale mOdelling of Refractory linings 764987 Grant. The authors from the University of Minho acknowledge the partial funding by FCT / MCTES through national funds (PIDDAC) under the R&D Unit Institute for Sustainability and Innovation in Structural Engineering (ISISE), under reference UIDB/04029/2020, and under the Associate Laboratory Advanced Production and Intelligent Systems ARISE under reference LA/P/0112/2020. This work is financed by national funds through FCT - Foundation for Science and Technology, under grant agreement 2021.05961.BD attributed to the first author.

REFERENCES

[1] M. Ali, T. Sayet, A. Gasser, E. Blond, Transient Thermo-Mechanical Analysis of Steel Ladle Refractory Linings Using Mechanical Homogenization Approach, Ceramics 2020, Vol. 3, Pages 171-189. 3 (2020) 171–188. https://doi.org/10.3390/ceramics3020016.

[2] P.N. Gajjar, P. Put, J.M. Pereira, B. Luchini, S. Sinnema, P.B. Lourenço, Characterisation of mortarless refractory masonry joints under elevated temperatures, Eng Struct. 275 (2023). https://doi.org/10.1016/J.ENGSTRUCT.2022.115234.

[3] R.L.G. Oliveira, J.P.C. Rodrigues, J.M. Pereira, P.B. Lourenço, H.U. Marschall, Thermomechanical behaviour of refractory dry-stacked masonry walls under uniaxial compression, Eng Struct. 240 (2021). https://doi.org/10.1016/j.engstruct.2021.112361.

[4] M. Ali, R.L.G. Oliveira, J.M. Pereira, J.P. Rodrigues, P.B. Lourenço, H. Ulrich Marschall, T. Sayet, A. Gasser, E. Blond, Experimental characterization of the nonlinear thermomechanical behaviour of refractory masonry with dry joints, Constr Build Mater. 364 (2023) 129960. https://doi.org/10.1016/J.CONBUILDMAT.2022.129960.

[5] A. Gasser, J. Poirier, Thermomechanical testing of a laboratory pilot containing refractory masonries without mortar, Open Ceramics. 13 (2023). https://doi.org/10.1016/J.OCERAM.2022.100325.

[6] P.N. Gajjar, M. Ali, T. Sayet, A. Gasser, E. Blond, J.M. Pereira, P.B. Lourenço, Numerical study on the nonlinear thermomechanical behaviour of refractory masonry with dry joints, Eng Struct. 291 (2023) 116468. https://doi.org/10.1016/J.ENGSTRUCT.2023.116468.

[7] S. Samadi, S. Jin, H. Harmuth, Combined damaged elasticity and creep modeling of ceramics with wedge splitting tests, Ceram Int. 47 (2021) 25846–25853. https://doi.org/10.1016/J.CERAMINT.2021.05.315.